# Phenomenological Model of Viscoelasticity for Systems Undergoing Sol-Gel Transition

Khushboo Suman,[1a] Sachin Shanbhag,[2*] and Yogesh M. Joshi[1*]

[1]Department of Chemical Engineering, Indian Institute of Technology Kanpur, Kanpur 208016, India

[2]Department of Scientific Computing, Florida State University, Tallahassee, Florida 32306

[a]Present address: Department of Chemical & Biomolecular Engineering, University of Delaware, Newark, DE 19716 USA

* Authors to whom correspondence should be addressed; electronic mail: sshanbhag@fsu.edu and joshi@iitk.ac.in

**Abstract**

A material undergoing sol-gel transition evolves from the pre-gel (sol) state to the post-gel state, through the critical gel state. It is well-known that critical gels exhibit power-law rheology. The faster decay of the relaxation modulus in the pre-gel state can be empirically described by modifying this power-law decay with a stretched exponential factor. A phenomenological analytical expression for the relaxation modulus in the post-gel state is proposed by invoking symmetry associated with the evolution of relaxation time on either side of the critical gel state, and by accounting for natural constraints. This expression, which depends on the extent of crosslinking, can be suitably transformed to obtain analytical expressions for the dynamic moduli and the continuous relaxation time spectrum. Thus, the proposed model facilitates a comprehensive description of viscoelastic evolution from the pre-gel to the post-gel states. It is validated by carrying out experiments on a model colloidal gel-forming system, and by considering other diverse gel-forming systems studied in the literature. After calibrating the parameters of the phenomenological model, it is found to be in excellent agreement with experimental data. Such a well-calibrated phenomenological model can be used to determine any linear viscoelastic response over a wide range of frequencies, and extents of crosslinking encompassing the entire sol-gel transition.

## 1. Introduction

Many colloidal and polymeric systems, subjected to certain stimuli (thermal, chemical, light, etc.) or otherwise, undergo spontaneous liquid to soft solid transition as a function of time. Among such transitions, an important category is the sol-gel transition.[1] Typical examples of such transition include crosslinking reactions in thermosetting polymers, adhesives, commercial gel-forming systems such as Carrageenan, colloidal gel-forming systems such as clay, Ludox®, food ingredients such as agar agar gel, etc.[2-11] During such a transition, gel-forming units (such as colloidal particles, polymeric precursors, etc.) form physical (van der Waals, electrostatic, depletion, etc.) or covalent bonds with each other. Accordingly, the cluster grows and in due course forms a space spanning percolated network that eventually undergoes densification. In the literature, much emphasis has been given to the percolated space spanning network state that corresponds to a fractal structure, which is also known as the critical gel state.[12-14] This is primarily because of the uniqueness associated with this state, wherein rheological response functions, for instance, dynamic moduli, relaxation modulus and creep compliance demonstrate power-law dependency on their respective independent variables, frequency or time.[15, 16] Comparatively less attention has been given to understanding how rheological properties evolve in the pre-gel and the post-gel state. In this paper, we analyze this topic theoretically and experimentally by considering different kinds of gel-forming materials.

A gel-forming material, in its sol state shows rheological properties of a viscous liquid wherein elastic ($G'$) and viscous ($G''$) moduli respectively show a quadratic and linear dependence on angular frequency ($\omega$) with ($G' << G''$). As gelation progresses, the cluster grows and the frequency dependence of both the moduli gets weaker with that of $G'$ getting weaker at a faster rate. At a certain point, the network percolates the space such that both the moduli show identical power-law dependence on frequency given by:[17]

$$G' = G'' \cot\left(n\pi/2\right) = \frac{\pi S}{2\Gamma(n)\sin\left(n\pi/2\right)}\omega^n, \tag{1}$$

where $n$ is the power-law exponent with $0 < n < 1$, $S$ the gel strength and $\Gamma$ is the Euler Gamma function. The identical power-law scaling of the dynamic moduli on frequency has also been confirmed by a microscopic framework for an attractive colloidal system.[18] This unique state has been termed as the critical gel state, where the percolated network is the weakest and has a fractal structure. Interestingly, the power-law dependence of the dynamic

moduli on the angular frequency with an exponent of $n$ is reflected in the evolution of all the other linear viscoelastic functions; the relaxation modulus and spectrum show inverse power-law dependence on time, while creep compliance shows a power-law increase with time, all with power-law exponent of $n$.[14, 19] As gelation progresses the dynamic moduli continue to get weaker with angular frequency but at a slower rate. During this process, the gel consolidates and becomes denser. In colloidal systems where spontaneous time dependent gelation process occurs, such as in clay systems, gel consolidation continues and the systems show out-of-equilibrium soft glassy dynamics.[20]

While the rheological response functions have been observed to demonstrate power-law rheology at the critical gel state, important observations have also been made regarding how other rheological functions vary as the critical state is approached from the pre-gel (sol) as well as the post-gel direction.[21] Particularly, it has been observed that viscosity diverges as the critical gel state is approached. In contrast, the equilibrium modulus (associated with zero frequency), which becomes finite beyond the critical gel state, grows in the post gel state. On the other hand, the relaxation time has been observed to diverge as the critical gel state is approached from either side, the pre-gel as well as the post-gel. These variables show power-law dependence on the distance to the critical gel point measured in terms of the degree of crosslinking.[21] The corresponding power-law exponents are related to each other in such a fashion that knowledge of $n$ and any other exponent leads to the estimation of all the remaining exponents.[19, 21]

Although the evolution of the viscosity, equilibrium modulus, and relaxation time is well-characterized by the scaling relations, knowledge of how the relaxation modulus, creep compliance and relaxation time spectrum evolve in the pre- and post-gel states is vital in order to have a better understanding of the rheological aspects of the gelation process. In an early attempt, Winter and coworkers[22] obtained the discrete relaxation time spectra by fitting a multimode Maxwell model to the dynamic moduli data at different extents of crosslinking. They considered identical exponential decay of relaxation modulus in the pre-gel and post-gel states except for the equilibrium modulus being non-zero in the post-gel state. However, this methodology depends on the number of modes, and the frequency window of the dynamic moduli data. In an important subsequent work, Scanlan and Winter[23] used critical exponents associated with the scaling laws and proposed a continuous function for the relaxation modulus in the pre-gel state. They modified the power-law decay of the relaxation modulus associated with the critical gel state by incorporating a stretched exponential function that

depends on the extent of crosslinking in the pre-gel state. This proposed functional form shows remarkable agreement with the experimental data of relaxation modulus in the pre-gel state. Scanlan and Winter[23] further speculated the possibility of extending the stretched exponential equation they proposed for the pre-gel state to the post-gel state by changing the argument of the exponential term from negative to positive and by incorporating the equilibrium modulus. Although such an approach could describe the transient response very close to the critical gel point, it could not describe their experimental observations at greater extents of crosslinking for a polydimethylsiloxane gel.[23] Furthermore, a stretched exponential function with a positive argument in the post-gel state results in the divergence of relaxation modulus at large times. Therefore, to the best of our knowledge, an appropriate form of the relaxation modulus in the post-gel state has not yet been established.

In this work, taking a cue from Winter and coworker's methodology,[23] we propose an analytical form for the relaxation modulus in the post-gel state. We also propose a systematic method for obtaining all the viscoelastic functions, and the relaxation time spectrum at different extents of crosslinking. Building on previous work, this leads us to a comprehensive phenomenological model that applies seamlessly from the pre-gel, through the critical, to the post-gel states. We validate this comprehensive model for distinctly diverse physically crosslinking gel systems, by carrying out new experiments as well as using the data from the literature.

## 2. Material, Sample Preparation and Experimental Protocol

We prepare an aqueous dispersion of a synthetic hectorite clay mineral, LAPONITE XLG®, a registered trademark of BYK Additives. The individual particles of LAPONITE XLG® are around 30 nm in diameter and 1 nm in thickness. Detailed information about the LAPONITE XLG® clay mineral can be found elsewhere.[24] Henceforth, we refer to this system as just clay. In this work, we prepare 3 weight % clay dispersion with 3 mM NaCl dispersion. The oven-dried clay (120°C for 4 h) is added to ultrapure water (Millipore, resistivity of 18.2 MΩ cm) having a predetermined quantity of salt. The solution is stirred continuously for a duration of 30 minutes using the IKA Ultra Turrax drive leading to a clear homogeneous dispersion. The freshly prepared samples are loaded in a shear cell to perform experiments. The rheological measurements are conducted using a TA Instruments DHR-3 rheometer with a sandblasted concentric cylinder geometry (cup diameter 30.38 mm and gap of 1.17 mm). We subject the sample to cyclic frequency sweep over a range of 0.5 – 25 rad/s

and at a constant oscillatory stress of 0.1 Pa within the linear viscoelastic limit. A single frequency sweep takes 100 s to complete, which is significantly less than the gelation time of the colloidal clay dispersion. We also estimate the mutation numbers, which have been observed to be always within the suggested limit ( $N'_{mu} = (2\pi/\omega G')(\partial G'/\partial t) < 0.1$ and $N''_{mu} = (2\pi/\omega G'')(\partial G''/\partial t) < N'_{mu}$ ). In all the experiments, the temperature is maintained at 10°C using the Peltier plate assembly. A thin layer of silicone oil is added on the free surface of the sample and a solvent trap is used to prevent the evaporation losses during the measurements.

### 3. Experimental Results

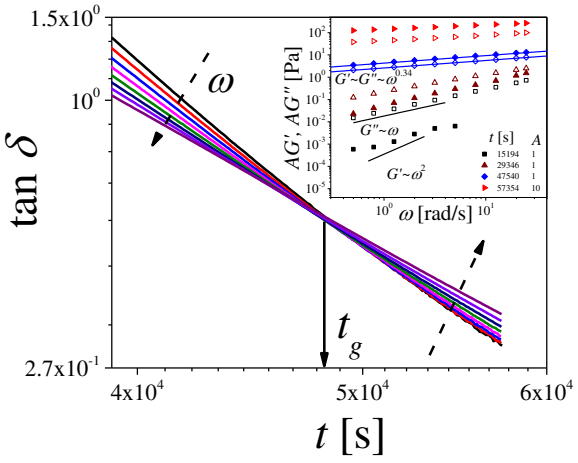


**Figure 1.** Evolution of $\tan\delta$ is plotted as a function of time at different frequencies over a range of 0.5 – 25 rad/s during the sol-gel transition in an aqueous dispersion of synthetic hectorite clay at 10°C. The dashed line indicates the direction of increasing angular frequency. The solid arrow denotes the point of independence of iso-frequency $\tan\delta$ curves. The inset shows the variation of $G'$ and $G''$ as a function of angular frequency at different extents of gelation. The value on the vertical axis has been shifted by a factor of $A$ for clarity. The solid blue line in the inset denotes the fit of Eq. 1.

Figure 1 describes the result of a cyclic frequency sweep experiment on the aqueous dispersion of clay at 10°C during the sol-gel transition. The dependence of elastic ($G'$) and viscous ($G''$) moduli on the angular frequency at different extents of gelation are shown in the inset of Figure 1. In the early stages of the gelation, the moduli exhibit liquid-like behavior, characterized by the presence of the terminal region. This indicates that the colloidal dispersion is in the sol state at early times. As time progresses, the moduli increase in magnitude but become less sensitive to frequency. Furthermore, $G'$ increases faster than $G''$. Eventually, at a certain time, $G'$ and $G''$ follow an identical power-law dependence on frequency, $G' \sim G'' \sim \omega^n$. The solid line represents the power-law dependence given by Eq. (1) with $S = 3.8$ Pas$^n$ and $n = 0.34$. With further increase in time, the dependence of moduli on frequency continues to weaken. The corresponding time evolution of loss tangent ($\tan\delta$) for the aqueous colloidal dispersion is plotted in Figure 1. The dashed line represents the direction of increasing $\omega$. As expected, $\tan\delta$ decreases with increasing frequency in the sol state. Very interestingly, the iso-frequency $\tan\delta$ curves intersect at a point and become independent of the applied frequency. The time corresponding to $\tan\delta$ becoming frequency-independent is known as the critical gelation time ($t_g$). At this point, the sample forms the weakest space spanning percolated fractal network. The corresponding value of the critical exponent ($n$) can be computed from the value of $\tan\delta$ at the critical point using the relation: $\tan\delta = \tan(n\pi/2)$. Expectedly, the computed value of $n$ is equal to the power-law exponent of moduli on frequency at the critical point. Such an equivalence validates the presence of the fractal network structure at the critical point according to the Winter criterion. For times greater than $t_g$, the dependence of $\tan\delta$ on $\omega$ reverses and $\tan\delta$ increases with $\omega$, which is a characteristic signature of the post-gel state. Therefore, Figure 1 clearly establishes that the colloidal dispersion undergoes spontaneous sol-gel transition at 10°C.

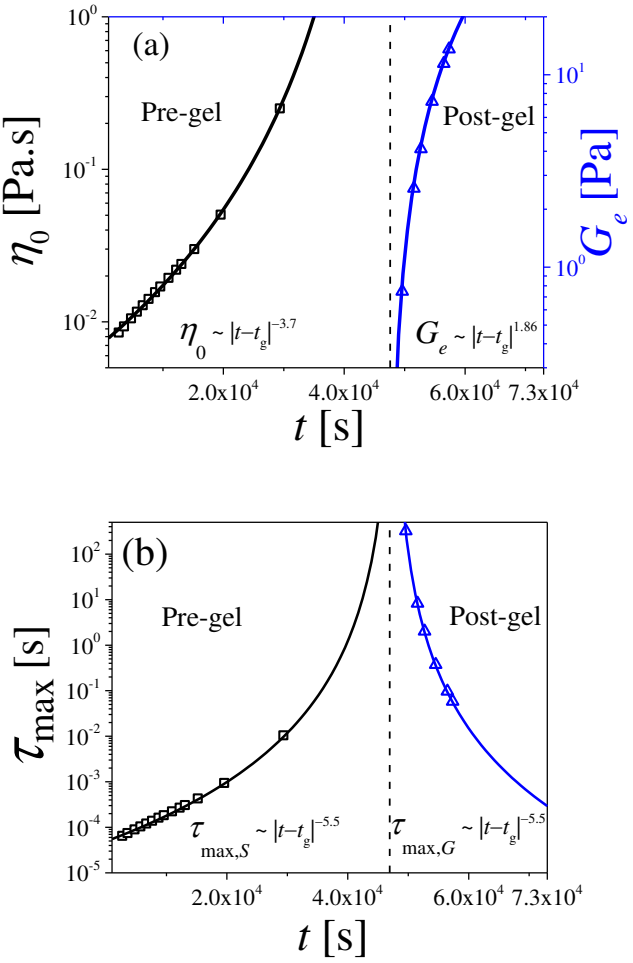


**Figure 2.** Evolution of (a) zero-shear viscosity ($\eta_0$), equilibrium modulus ($G_e$) and (b) longest relaxation time in the pre-gel state ($\tau_{max,S}$) and in the post-gel state ($\tau_{max,G}$) are plotted as functions of time for colloidal dispersion of hectorite clay undergoing sol-gel transition at 10°C.

The results of the dynamic mechanical measurements enable the estimation of the various other rheological properties such as relaxation time, viscosity and equilibrium

modulus during the sol-gel transition. The zero-shear viscosity and the equilibrium modulus are associated with the zero-frequency limit and the relaxation time is obtained as the inverse of the frequency associated with the point of intersection of low frequency and high-frequency asymptotes. A detailed procedure to systematically estimate these parameters is discussed elsewhere.[19, 21] In Figure 2, we plot the evolution of zero-shear viscosity ($\eta_0$) and longest relaxation time ($\tau_{\max,S}$) in the pre-gel state and equilibrium modulus ($G_e$) and longest relaxation time ($\tau_{\max,G}$) in the post-gel state as a function of time for colloidal clay dispersion at 10°C. As time increases, the clay particles engage in interparticle bond formation. This results in the formation of clusters that grow in size as time progresses. In the pre-gel state, the increase in the cluster size is marked by the simultaneous increase of both $\eta_0$ and $\tau_{\max,S}$. At the point of critical gel transition, some of the growing clusters coalesce to form a space-spanning percolated structure. This causes the divergence in both $\eta_0$ and $\tau_{\max,S}$ as shown in Figure 2. Beyond the critical gel state, the system no longer shows a zero-shear rate viscosity. The percolated network is the weakest at the critical point. Gradually, the remaining free clusters join the percolated network. During this phase, larger free clusters are more likely to be recruited than the smaller ones. Consequently, in the post-gel state, the longest relaxation timescale – that corresponds to the relaxable components like unattached particles/clusters – decreases with an increase in time. Simultaneously, the system shows an equilibrium modulus suggestive of solid-like behavior of the network as a whole. At the point of critical gel transition, the value of equilibrium (zero frequency) modulus $\left(G_e\right)$ is 0 and as the gel consolidates, it increases with time in the post-gel state as shown in Figure 2(a).

For polymeric gels, it has been observed that $\eta_0$, $G_e$, $\tau_{\max,S}$ and $\tau_{\max,G}$ show a power-law dependence on extent of crosslinking ($\tilde{p}$), given by $\left(\tilde{p} = \left|p - p_c\right|\right)$, where $p$ is the degree of crosslinking expressed as the fraction of crosslinkable monomeric units participating in the network, with $p_c$ as the degree of crosslinking at the critical gel state.[25] The reported relations are given by:[25, 26]

$$\eta_0 \sim \left|p - p_c\right|^{-s} \tag{2}$$

$$G_e \sim \left|p - p_c\right|^{z} \tag{3}$$

$$\tau_{\max,S} \sim \left|p - p_c\right|^{-\nu_S} \tag{4}$$

$$\tau_{\max,G} \sim \left|p - p_c\right|^{-\nu_G} \tag{5}$$

Interestingly, the critical exponents associated with relations given by Eqns. (2) to (5) are observed to be interrelated as:[21]

$$\nu_S = \frac{s}{(1-n)} \text{ and} \tag{6}$$

$$\nu_G = \frac{z}{n}. \tag{7}$$

The above expressions are also known as hyperscaling relations. Since the sol-gel transition occurs spontaneously in the clay dispersion, we expect viscoelastic parameters to scale with a relative distance to gelation expressed in terms of time ($\tilde{t} = \left|t - t_g\right|$). Consequently, we fit scaling laws given by Eqns. (2) to (5) with $\left|p - p_c\right|$ replaced by $\left|t - t_g\right|$. The corresponding fit of the scaling laws to the experimental data is shown in Figure 2 by the solid line. It can be seen that the scaling laws are in excellent agreement with the experimental data. The fits to these scaling laws lead to the estimation of the scaling exponents as $s$ = 3.7, $z$ = 1.86, $\nu_S$ = 5.5, and $\nu_G$ = 5.5. It is important to note that the scaling exponents are not independent to take any value and are interrelated by the hyperscaling laws.[19] Interestingly, the scaling exponents associated with the growth of $\eta_0$ and $G_e$ have also been estimated theoretically. Using the classical Flory-Stockmayer framework, Gordon and Ross-Murphy[27] estimated $z$ = 3. Within percolation theory, the scaling exponent $z$ has been determined by drawing an analogy between the conductance of random resistor networks and the elastic modulus in a nascent gel. Based on this approach, numerical estimates of $z$ = 1.5,[28] and analytical estimates around $z$ = 1.7 can be obtained.[26, 29] Using a different approach within percolation theory, Martin *et al.*[30] obtained $z$ = 2.66, and $s$ = 1.33. It is also possible to make connections to more general theories that seek to explain the origin of elastic modulus in amorphous materials. These approaches may be classified into two broad frameworks: rigidity percolation and nonaffine displacement. In the former, an amorphous solid is visualized as a mixture of rigid and floppy domains.[31] As the mean coordination of an atom increases, rigidity percolates through the network and a modulus emerges. He and Thorpe[32] numerically modelled covalent glasses as continuous random networks and systematically increased the average number of bonds per atom. Beyond a critical threshold, they observed the emergence of a non-zero elastic modulus whose

magnitude increased with distance from the critical point with an exponent $z$ = 1.5. An alternative framework traces the emergence of elastic modulus to nonaffine atomic displacements in disordered lattices that characterize amorphous solids.[33] With this approach, a value of $z$ = 1 was analytically obtained using an approximate mean-field theory. Subsequently, a connection between the two frameworks was discovered, which integrated the ideas of rigidity percolation and nonaffine displacement.[34] Differences between the values of $z$ obtained from the two approaches were attributed to non-mean-field correlations near the rigidity transition. To summarize, the scaling exponents are not universal constant as evident from experiments and theoretical studies, although they are interrelated with each other.[19]

Another important aspect of the experimental computed critical exponents is that the evolution of relaxation time in the neighbourhood of the critical gel state has been observed to be symmetric leading to: $\nu_S = \nu_G$. In addition to this work, numerous other studies on different physically and chemically crosslinking systems also suggest $\nu_S = \nu_G$.[19, 35, 36] Interestingly the inverse of these exponent: $\nu_S^{-1} = \nu_G^{-1} = \kappa$ is the dynamic critical exponent, which has been experimentally observed to take values in a narrow range of 0.17 – 0.3.[19, 37] Furthermore, the very fact that $\nu_S = \nu_G$, leads to: $n = z/(z+s)$.[21] This theoretical analysis and experimental observation appear to be independent of the nature of the gelation (physical or chemical), gel-forming system (polymeric or colloidal), concentration, and experimental conditions like temperature environment.[19] Importantly, these scaling exponents show an excellent agreement with the hyperscaling relations given by Eqns. (6) and (7) including $\nu_S = \nu_G$, which implies $n = z/(z+s)$. For the colloidal dispersion explored in the present work, the computed value of $\kappa$ = 0.19 lies within the prescribed range. Importantly such an equivalence corroborates that $|t - t_g|$ is related to the distance from the critical gel state $|p - p_c|$ as:

$$|t - t_g| \sim |p - p_c|. \tag{8}$$

The above correspondence has also been verified for many spontaneous (time-dependent) physical as well as chemical gel-forming systems.[23] In general, it has been observed that if $R$ is the parameter that controls the extent of gelation, such that $R_c$ is associated with the

critical gel state, $|p-p_c| \sim |R-R_c|$.[3, 36] In this work, we discuss systems wherein the degree of gelation gets controlled by time, temperature as well as concentration.

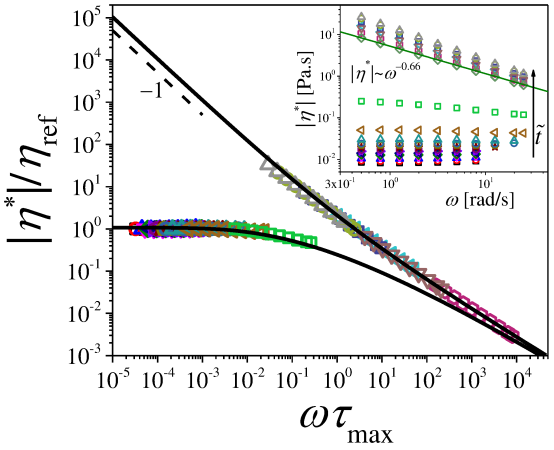


**Figure 3.** Normalized complex viscosity $|\eta^*|$ is plotted as a function of $\omega\tau_{max}$ for colloidal dispersion of clay at 10°C. The experimental data is shown by symbols and the fitted model is shown by lines. The dashed line denotes a slope of $-1$. The inset shows the variation of $|\eta^*|$ as a function of $\omega$ at increasing extent of gelation $|t-t_g|$ in the colloidal dispersion. The solid line in the inset represents the power-law decay of $|\eta^*|$ at the critical gel state with an exponent of $n-1=-0.66$.

In order to gain further understanding about the evolution of the viscoelastic behavior of the colloidal dispersion during the sol-gel transition, we plot the complex viscosity $|\eta^*|$ as a function of $\omega$ in the inset of Figure 3. At early stages of crosslinking, $|\eta^*|$ exhibits a plateau over the explored range of frequency. With an increase in the extent of gelation, it can be seen that the plateau value of $|\eta^*|$ is limited to low $\omega$ and is accompanied by $\omega$ dependent decrease. At the point of critical gel transition, $|\eta^*|$ exhibits a power-law dependence on $\omega$ given by $|\eta^*| \sim \omega^{n-1}$. The power-law fit of $|\eta^*|$ as given by Eq. (1), is

represented by a solid line in the inset of Figure 3. Remarkably, the observed power-law exponent is identical to the theoretical value of $n-1$. In the post-gel state, the value of $|\eta^*|$ increases further and exhibits an inverse $\omega$ dependence in the limit of low $\omega$. Such a dependence is suggestive of a solid-like response. Using the computed values of $\eta_0$, $G_e$, $\tau_{\max,S}$ and $\tau_{\max,G}$, we obtain a unique superposition of $|\eta^*|$ using the protocol suggested by Winter.[21] In Figure 3, we plot $|\eta^*|$ normalized by a reference viscosity $(\eta_{\text{ref}})$ as a function of $\omega\tau_{max}$. In the pre-gel region, $\eta_{\text{ref}}$ is taken as $\eta_0$ and $\tau_{max}$ is taken as $\tau_{\max,S}$, while in the post-gel region, $G_e\tau_{\max,G}$ serves as $\eta_{\text{ref}}$ and $\tau_{\max,G}$ as $\tau_{max}$. It can be seen that the viscosity data collapse into two exclusive curves for the pre-gel and the post-gel states. It is important to note that the shift factors leading to the superposition are not arbitrary, instead, they are uniquely determined by the parameters $\eta_0$, $G_e$, $\tau_{\max,S}$ and $\tau_{\max,G}$ described in Figure 2.

In the pre-gel state, the normalized $|\eta^*|$ achieves a plateau in the limit of low $\omega$, which is followed by a frequency-dependent decrease. On the other hand, the nature of the curve in the post-gel state is very different from the pre-gel state. It does not plateau at low frequency; instead, the normalized viscosity exhibits a power-law decrease with a slope of $-1$ as shown by the dashed line. Interestingly, the behavior of the pre-gel and post-gel states at high-frequency approaches the power-law behavior of the critical gel state.

The unique superposition of $|\eta^*|$ in the pre-gel and post-gel states leads to remarkable consequences. Similar to time-temperature superposition in polymeric systems, the superposition of $|\eta^*|$ using these scaling laws expands the window of experimentally accessible timescales (4 – 6 decades in Figure 3, instead of approximately two decades in the inset). It also implies that the shape of the relaxation time spectrum is preserved (separately) in the pre-gel and the post-gel states. Taken together, there is a strong incentive to develop a comprehensive linear viscoelastic model that describes the sol-gel transition. Such a model, adequately calibrated with superposed experimental data, would be able to describe the rheological response from arbitrarily small to large timescales. As a corollary, the hyperscaling laws generalize the ability to completely describe the rheology at a particular extent of gelation, to arbitrary extents of gelation.

**4. Development of the Phenomenological Model**

The oscillatory experiment results lead to the estimation of the scaling exponents, which suggests a simple power-law evolution for the viscoelastic parameters in the pre-gel and the post-gel state. Furthermore, we expect these scaling exponents to characterize other dynamic viscoelastic properties as well. At the critical gel state, the stress relaxation modulus $G(t)$ of a critical gel exhibits a power-law decay with respect to time given by:[38]

$$G(t) = St^{-n}. \tag{9}$$

The above equation can be obtained by taking an inverse Fourier transform of the dynamic moduli given in Eq. (1). Moreover, experimentally, colloidal and polymeric gel-forming systems routinely show such behavior at the critical point.[38, 39] In an attempt to describe the evolution of the relaxation modulus at all extents of crosslinking for a pre-gel state, Scanlan and Winter[23] proposed the following generic form:

$$G(t,p) = G(t,p_c) f\left[\frac{t}{\tau_{\max,S}}\right], \tag{10}$$

where $G(t,p_c)$ is the evolution of the relaxation modulus at the critical gel state and $f\left[\frac{t}{\tau_{\max,S}}\right]$ is the cut-off function. On substituting the dependence of $G$ given by Eq. (9) and the divergence of $\tau_{\max,S}$ given by Eq. (4) in the above equation, we get:[23]

$$G(t,p) = St^{-n} f\left(\frac{t}{\bar{C}_S |p_c - p|^{-1/\kappa}}\right), \tag{11}$$

where $\bar{C}_S$ is the constant of proportionality associated with the scaling equation of $\tau_{\max,S}$. While the form of the cut-off function needs to be determined experimentally, a stretched exponential function has been observed to describe the behavior quite well in the pre-gel state.[39-41] On adopting a stretched exponential form for the cut-off function given by $f(x) = exp(-x^{\kappa})$, $G(t,p)$ can be expressed as:[23]

$$G(t,p) = St^{-n} \exp\left(-\left(\frac{t}{\bar{C}_S |p_c - p|^{-1/\kappa}}\right)^{\kappa}\right). \tag{12}$$

In the expression of $f(x)$, $\kappa$ is used as the stretching exponent to avoid the divergence of the derivative of $G$ at $p_c$. Simplification of Eq. (12) leads to:

$$G(t,p) = St^{-n}\exp\left(-\alpha_S t^{\kappa}\right), \tag{13}$$

where $\alpha_S = |p_c - p|/\bar{C}_S^{\kappa}$. The faster relaxation expected in the pre-gel state (associated with $\alpha_S > 0$) of various gel-forming materials is well-described by Eq. (13).[22]

From the apparent symmetry in the mathematical structure and experimental observations of symmetry in the divergence of the longest relaxation time in the vicinity of the critical point, it is tempting to hypothesize a stretched exponential form given by $G(t,p) = St^{-n}\exp\left(\alpha_G t^{\kappa}\right)$, with $\alpha_G \sim (p - p_c)$, as the form associated with generic material behavior in the post gel state. Interestingly, for small values of $t$, this expression describes experimental data of relaxation modulus reasonably well. However, as time $t$ increases, there is a competition between the power-law decrease associated with term $t^{-n}$ and the exponential increase associated with the term $\exp\left(\alpha_G t^{\kappa}\right)$. At small $t$, the $t^{-n}$ term dominates so that $dG/dt < 0$. However, beyond a threshold marked by $t^* = (n/\alpha_G\kappa)^{1/\kappa}$, the exponential term dominates, and $dG/dt > 0$, which is unphysical for a relaxation modulus.

The above-mentioned inevitable aspect is due to the fact that the exponential function grows faster than any power-law function, because the Maclaurin or Taylor series of an exponential function is an infinite sum of power-laws of increasing strength. In order to reconcile (i) the observation that at short times the exponential functional form works well, and (ii) the monotonicity required of a physically sensible relaxation modulus ($dG/dt \le 0$), we entertain a compromise in which the Maclaurin series for the exponential function is truncated after $m+1$ terms:

$$e^{\alpha_G t^{\kappa}} = \sum_{l=0}^{\infty}\frac{(\alpha_G t^{\kappa})^l}{l!} \approx 1 + \alpha_G t^{\kappa} + \cdots + \frac{\alpha_G{}^m t^{m\kappa}}{m!}. \tag{14}$$

Note that at short times ($t << t^*$), $\alpha_G t^{\kappa}$ is small, and the truncated series is an excellent approximation consistent with experimental observations. If we select $m < n/\kappa$ so that the highest order term ($t^{m\kappa}$) does not overwhelm $t^{-n}$, we can ensure monotonicity of the

relaxation modulus for the post-gel state. Together, this leads us to conjecture a form for $m$ given by:

$$m = \text{floor}\left(\frac{n}{\kappa}\right), \tag{15}$$

where $\text{floor}(x)$ is the largest integer that is not greater than $x$. For the clay gel used in the present work, $\kappa \approx 0.18$ and $n \approx 0.34$, implies $m = 1$. If $\kappa \approx 0.2$ and $n \approx 0.5$, we get $m = 2$. The expression proposed for $m$ in Eq. (15) guarantees $dG/dt \leq 0$, while maximizing the range of $t$ over which the truncated form approximates the underlying exponential function. While the proposed $G(t, p)$ for the post-gel satisfies necessary constraints and incorporates empirical observations, it is entirely conjectural at this point. It remains to be seen whether it is sufficient to quantitatively describe the evolution of viscoelasticity in the post-gel state observed in experiments.

Nevertheless, we can now summarize the proposed comprehensive phenomenological model for the relaxation modulus of a system undergoing sol-gel transition as:

$$G(t) = St^{-n}e^{-\alpha_S t^{\kappa}} \qquad \text{Pre-gel} \tag{16}$$

$$G(t) = St^{-n} \qquad \text{Critical Gel} \tag{17}$$

$$G(t) = St^{-n}\left(1 + \alpha_G t^{\kappa} + \cdots + \frac{\alpha_G^m t^{m\kappa}}{m!}\right) + G_e \qquad \text{with } m = \text{floor}\left(\frac{n}{\kappa}\right) \quad \text{Post-gel} \tag{18}$$

The expressions associated with pre-gel and critical gel states have been previously reported in the literature.[14, 23] Interestingly, the power-law decay of relaxation modulus at the critical gel point is uniquely determined by the critical gel parameters $S$ and $n$. Similar to the critical gelation point, Milkus and Zaccone[42] theoretically estimate a power-law decay in the vicinity of the isostatic point for central-force lattices. Such power-law dependence is attributed to the interplay between nonaffine dynamics and soft vibrational modes in disordered solids. Importantly, the expression associated with the post-gel state is the main contribution of the present work. It can be seen that the six parameters, $S$, $n$, $\kappa$, $G_e$, $\alpha_S$ and $\alpha_G$ completely describe the relaxation modulus over the entire range of the sol to gel transition. Three of these parameters, $S$, $n$, and $\kappa$, are distinctive features of the critical gel state and can be obtained from any linear viscoelastic experiment on the critical gel state.

Particularly, the parameters $S$ and $n$ can be computed using Eq. (1), while $\kappa$ describes the evolution of the relaxation timescale in the vicinity of the critical gel state and can be estimated from Eqns. (4) and/or (5) with $\nu_S^{-1} = \nu_G^{-1} = \kappa$.

Out of the other three parameters, $\alpha_S$ is associated with the sol or pre-gel state, while $G_e$ and $\alpha_G$ are associated with the post-gel state. Unlike $S$, $n$ and $\kappa$, these remaining parameters ($\alpha_S$, $\alpha_G$ and $G_e$) are not constant, but depend on the extent of gelation. At a given extent of crosslinking $G_e$ can be obtained experimentally as demonstrated in Figure 2. Furthermore, $\alpha_S$ and $\alpha_G$ are natural gelation variables that are proportional to the distance from the critical gel state in terms of degree of crosslinking $\left(\left|p_c - p\right|\right)$. They can be extracted by selecting a reference value of $\left|p_c - p\right|$ in the pre-gel and post-gel state, and calibrating the phenomenological model to superposed experimental observations of any linear viscoelastic response function (dynamic moduli, complex viscosity, relaxation modulus, creep compliance, etc.) This reference value of $\left|p_c - p\right|$ serves the same role as the reference temperature in time-temperature superposition. Once $\alpha_S$ and $\alpha_G$ are determined for the "reference state", they can be used to obtain the response at any other value of $\left|p_c - p\right|$ using the hyperscaling laws.

For the experimental system reported in the previous section, the degree of crosslinking is represented in terms of time such that $\left|p_c - p\right| \sim \left|t_g - t\right|$. Thus, the parameters $\alpha_S$ and $\alpha_G$ are proportional to $\left|t - t_g\right|$ as $\alpha_S = \left|t_g - t\right| / C_S^{\kappa}$ and $\alpha_G = \left|t_g - t\right| / C_G^{\kappa}$, wherein the constants $C_S$ and $C_G$ are unknown. Thus, when we calibrate the model given by Eqns. (16) to (18) with experimental data at a particular reference state, we effectively determine the constants $C_S$ and $C_G$.

After selecting a reference state, the value of $G_e$ is predetermined using the scaling relation and the only fitting parameters are $\alpha_S$ and $\alpha_G$. The method that we adopt to determine them and hence calibrate the phenomenological model is mentioned below. We guess initial values of $\alpha_S$ and $\alpha_G$, and use the model given by Eqns. (16) to (18) to obtain

$G(t)$ from these parameters. The relationship between the relaxation spectrum $H(\tau)$ and $G(t)$ is given by:[43-45]

$$G(t) = G_e + \int_{-\infty}^{\infty} H(\tau) e^{-t/\tau} d\log\tau \tag{19}$$

For pre-gels, we extract the relaxation spectrum from the relaxation modulus through Eq. (19) using the "pyReSpect-time" program; the underlying method is described in detail elsewhere.[46] It uses non-linear Tikhonov regularization with a Bayesian criterion to infer $H(\tau)$ from $G(t)$ using Eq. (13). Once $H(\tau)$ is extracted, it is straightforward to compute $G^*(\omega)$ using relationships given by:[43-45]

$$G'(\omega) = G_e + \int_{-\infty}^{\infty} H(\tau) \frac{\omega^2\tau^2}{1+\omega^2\tau^2} d\log\tau \text{ and} \tag{20}$$

$$G''(\omega) = \int_{-\infty}^{\infty} H(\tau) \frac{\omega\tau}{1+\omega^2\tau^2} d\log\tau\,. \tag{21}$$

The complex viscosity can then be obtained as:[45]

$$\left|\eta^*(\omega)\right| = \frac{\sqrt{G'^2 + G''^2}}{\omega}. \tag{22}$$

In the pre-gel state, the complex viscosity cannot be obtained analytically from the relaxation modulus; instead it has to be determined numerically. Interestingly, for the critical gel state, the power-law decay of relaxation modulus, represented by Eq. (17), leads to the estimation of continuous relaxation time spectrum given by:[14]

$$H(\tau) = \frac{S}{\Gamma(n)} \tau^{-n}\,. \tag{23}$$

For the post-gel state, on the other hand, the proposed form given by Eq. (18) leads to an analytical estimation of $H(\tau)$, $G^*(\omega)$ and hence $\left|\eta^*\right|$. In the expression for $G(t)$, we can interpret the terms in the summation as components that mathematically resemble the relaxation modulus of critical gels as:

$$G(t) = G_e + \sum_{i=0}^{m} \frac{\alpha_G^i S}{i!} t^{-(n-i\kappa)}. \tag{24}$$

Due to the linearity of Eq. (18) and Eq. (19), the spectra can also be visualized as a sum of contributions given by:

$$H(\tau)=\sum_{i=0}^{m}\frac{\alpha_G^i S}{\Gamma(n-i\kappa)}\tau^{-(n-i\kappa)}\,, \tag{25}$$

It should be noted that each of the terms in the sum of $H(\tau)$ given by Eq. (25) corresponds to the respective component in the sum associated with $G(t)$ given by Eq. (24). Extending the same concept, the dynamic moduli $G'$ and $G''$ can also be obtained as a sum of $m+1$ components given by:

$$G'(\omega)=G_e+\sum_{i=0}^{m}\frac{S_i\omega^{n_i}}{\Gamma(n_i)}\frac{\pi}{2}\operatorname{cosec}\left(\frac{n_i\pi}{2}\right) \text{ and} \tag{26}$$

$$G''(\omega)=\sum_{i=0}^{m}\frac{S_i\omega^{n_i}}{\Gamma(n_i)}\frac{\pi}{2}\sec\left(\frac{n_i\pi}{2}\right). \tag{27}$$

Finally, with the knowledge of dynamic moduli, the complex viscosity $|\eta^*|$ can be estimated analytically from Eq. (22) for the post-gel state. To summarize, given a set of six parameters, we can estimate the complex viscosity $|\eta^*|$ corresponding to the phenomenological model numerically for the pre-gel state, and analytically for the post-gel state.

**5. Results and Discussion**

Before we can fit the superposed experimental data shown in Figure 3, we have to select reference "extent of gelation" for the pre-gel and post-gel states. We use the $|t_g-t|$ corresponding to $\tau_{\max,S}=1$ s as the reference value for the pre-gel state. We use the same value of $|t_g-t|$ = 7920 s as the reference for the post-gel state. However, the choice of what reference state to use in the pre-gel and post-gel states is arbitrary. With the knowledge of $|t_g-t|$ and the scaling relations given by Eqns. (2) to (5) expressed in terms of time, $\tau_{\max,G}$, $\eta_0$ and $G_e$ used to normalize $|\eta^*|$ are obtained as 0.18 s, 5.47 Pa.s and 9.14 Pa respectively. The unknown parameters $\alpha_S$ and $\alpha_G$ are obtained by fitting the normalized $|\eta^*|$ obtained

from the phenomenological model to the experimental data. In practice, we additionally allow some of the known parameters ($\kappa$, $S$ and $n$) to vary slightly (within 10% of their originally determined values) and minimize the absolute value ('soft_l1' loss function) of the difference between the experimental and theoretical curves using the non-linear least-squares routine (least_squares) from the optimization package in SciPy.[46]

The normalized $|\eta^*|$ obtained from fitting or calibrating of the model are plotted as solid lines in Figure 3. It can be seen that $|\eta^*|$ obtained from $G$ given by Eqns. (16) to (18) describes the experimental data remarkably well. Such an agreement provides initial validation for the functional form of $G$ conjectured in Eqns. (16) to (18) for the pre-gel and post-gel states. This is particularly remarkable for the post-gel state, where the form of the relaxation modulus was proposed based solely on symmetry and physical constraints. Furthermore, such a model-based description of complex viscosity has important consequences: (i) the model prediction of complex viscosity is no longer limited by the frequency range of the observations, and (ii) it allows extrapolation to frequencies that are otherwise experimentally inaccessible. The low-frequency asymptote, which is otherwise not practical to explore via rheometry, is clearly evident. The high-frequency asymptote can also be seen approaching the power-law behavior in the pre-gel and post-gel states.

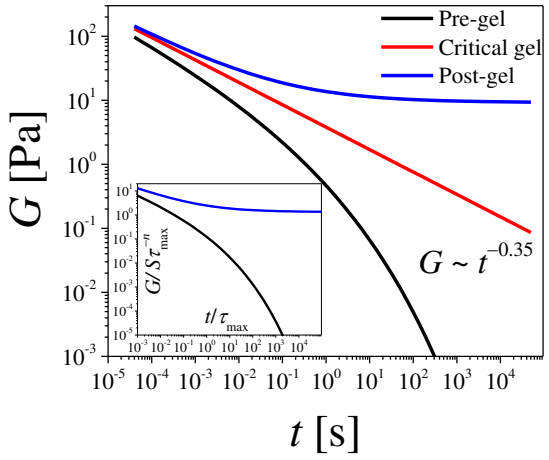

**Figure 4.** The evolution of relaxation modulus ($G$) in the pre-gel, critical gel and post-gel state is plotted as a function of time. The inset shows the same data for the pre-gel and post-gel state on a dimensionless scale.

**Table 1.** Model parameters used to define $G(t)$ for the colloidal dispersion undergoing sol-gel transition at 10°C.

| Model Parameter | Value | Source |
|---|---|---|
| $n$ | 0.35 | Figure 1, Eq.1 |
| $S$ | 3.8 Pa.s$^n$ | Figure 1, Eq.1 |
| $\kappa$ | 0.19 | Figure 2, Eq. 4, 5 |
| $\alpha_S$ | 2.1 [$1/s^\kappa$ ] | Fit |
| $\alpha_G$ | 0.2 [$1/s^\kappa$ ] | Fit |
| $G_e$ | 9.14 Pa | Figure 2, Eq. 3 |

After fitting the model to the complex viscosity, all the parameters of the model are established. These are listed in Table 1. Using these parameters, we now plot the evolution of relaxation modulus given by Eqns. (10) - (12) in the pre-gel, critical gel and post-gel states in Figure 4. As expected, $G$ associated with the pre-gel state corresponding to a particular $|t-t_g|$ decreases exponentially and relaxes to 0. The zero-shear viscosity obtained by integrating $G(t)$ is equal to $\eta_0$ = 4.65 Pa.s obtained experimentally for the pre-gel reference state. This is the same $\eta_0$ used to normalize the complex viscosity for this $|t-t_g|$ in Figure 3. At the point of the critical gel transition, $G$ follows a power-law decay with an exponent given by $n$. This suggests that stress can ideally relax to zero at infinite time. Beyond the gel point as the crosslinking increases, $G$ grows and the relaxation times become noticeably longer than the pre-gel state. However, the decay of $G$ becomes progressively sluggish for the post-gel state and approaches a plateau at very long times in the log-log plot. The finite value of relaxation modulus at very large times is the terminal plateau modulus (equilibrium modulus) of the gel associated with the post-gel reference state. The value of $G$ can be nondimensionalized using $S\tau_{\max}^{-n}$ in the pre-gel and the post-gel state and is plotted as a function of nondimensionalized time ($t/\tau_{\max}$) in the inset of Figure 4.

Such dependence of relaxation modulus in the pre-gel, critical gel and post-gel states has been observed for various polymeric crosslinking materials.[39, 47] With the established form of $G$ in the pre-gel and post-gel state given by Eq. (10) to (12), it is now possible to predict the evolution of $G$ at any extent during the crosslinking process by simply scaling the prefactors $\alpha_S$ and $\alpha_G$ of the exponential term. For early stages of crosslinking, the material relaxes rapidly, which is beyond the detection limit of the rheometer. However, with the model proposed in this work, it is now possible to predict the evolution of relaxation modulus for early stages of crosslinking. Furthermore, one can get an entire spectrum of the evolution of relaxation modulus in the pre-gel and post-gel states without conducting extensive experiments.

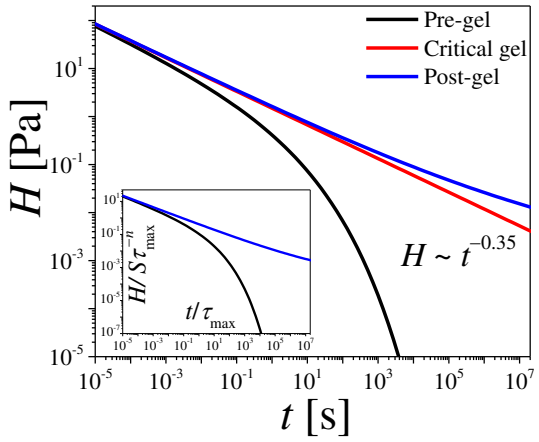


**Figure 5.** The relaxation spectra ($H$) for the colloidal dispersion undergoing sol-gel transition. The inset shows the same data for the pre-gel and post-gel state on a dimensionless scale.

With the computation of all the model parameters of the proposed model for relaxation modulus Eq. (13), we extract the relaxation time spectrum. For the pre-gel state, we obtain $H$ using the pyReSpect-time program[48] while for the post-gel state, we obtain $H$ analytically as described previously. The computed relaxation time spectrum is plotted in Figure 5 and the inset shows the evolution in a nondimensionalized scale. For the pre-gel

state, it can be seen that the smaller relaxation modes are heavily populated while the larger relaxation modes are scarce. This suggests that the relaxation time of the pre-gel state is very short since the precursor units of crosslinking have not yet participated in the cluster formation. At gel point, $H$ follows a power-law dependence with the decay rate dictated by $n$. Such dependence suggests the same behavior in the relaxation of stress at all scales of observation.[14] The negative value of the power-law exponent suggests that the fast relaxation modes dominate the gel structure and the slow modes are fewer in number. Interestingly, the power-law spectrum at the critical gel state has been found to be obeyed by a wide range of physical and chemical gels.[5, 49, 50] Beyond the gel point, the population of the longer relaxation times increase as the smaller unattached clusters participate in the percolated network. It is important to note that while the longest relaxation timescale associated with the relaxable components diverge symmetrically in the vicinity of the critical point, the relaxation spectrum of the post-gel state as a whole is not simply a reflection of the pre-gel state. The relaxation is distinctively different in the pre-gel and post-gel. This is an important result which for the first time reports the relaxation time spectrum of a gel-forming system at various stages of gelation.

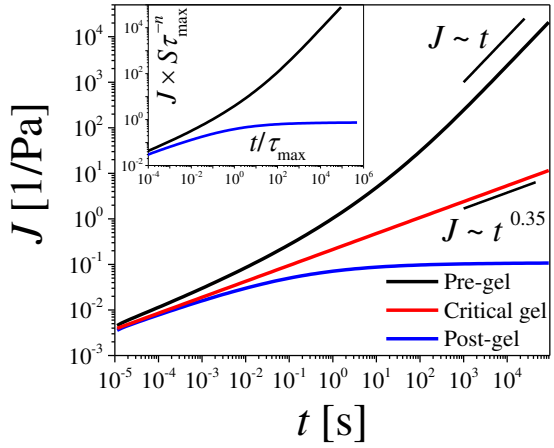


**Figure 6.** Evolution of creep compliance ($J$) as a function of time for the colloidal dispersion. The inset shows the same data for the pre-gel and post-gel state on a dimensionless scale.

With the knowledge of the various viscoelastic properties $G$, $H$, $|\eta^*|$ from the model, we now aim to obtain the creep compliance ($J$) from the proposed model for $G$. The conversion of $G$ to $J$ is a long-standing problem in polymer rheology, with two categories of widely applied methods. In the first category, a discrete relaxation spectrum (Prony series) is obtained from $G$, which is then transformed to a discrete retardation spectrum from which $J$ can be obtained.[51, 52] The second category of methods uses the convolution relation:[45]

$$t = \int_0^t G(t-t')J(t')dt', \tag{28}$$

to numerically obtain $J(t)$ from $G(t)$ at (potentially unevenly spaced) discrete times $[t_0, t_1, \cdots t_N]$.[53-55] Here, we follow the latter approach but exploit knowledge of the functional dependence of $G(t)$ on model parameters to evaluate some of the intermediate integrals analytically. The method is described in Appendix A.

The numerically computed $J$ from $G$ is plotted as a function of time in Figure 6 for the pre-gel, critical gel and post-gel state. For the pre-gel state, in the limit of large times $J$ increases linearly with time, which signifies the dominant viscous nature of the pre-gel state. At the point of critical gel transition, $J$ increases in a power-law fashion, which is a characteristic behavior of the critical gel state. Beyond the critical gel point, the rate of increase in $J$ decreases with time. Similar to the plateau in $G$ in Figure 5, $J$ eventually reaches a plateau.

With the proposed model for $G$, we are now able to construct a systematic way to estimate the various viscoelastic properties of a gel-forming system at different stages of gelation. Most importantly, the estimation of the relaxation time spectrum, which has been a challenging task in the field of soft matter rheology, is now analytically estimated with the proposed form of $G$ in the post-gel state. Furthermore, the relaxation time spectrum renders new insights about the contribution of the different relaxation modes. Additionally, on conducting only one oscillatory experiment and using the proposed model for $G$, we are also able to predict the behavior of the gel-forming material subject to the creep flow field. Therefore, on performing one experiment, we are able to obtain different viscoelastic functions which characterize the gel-forming system quite well.

**6. Wide Applicability of the Model**

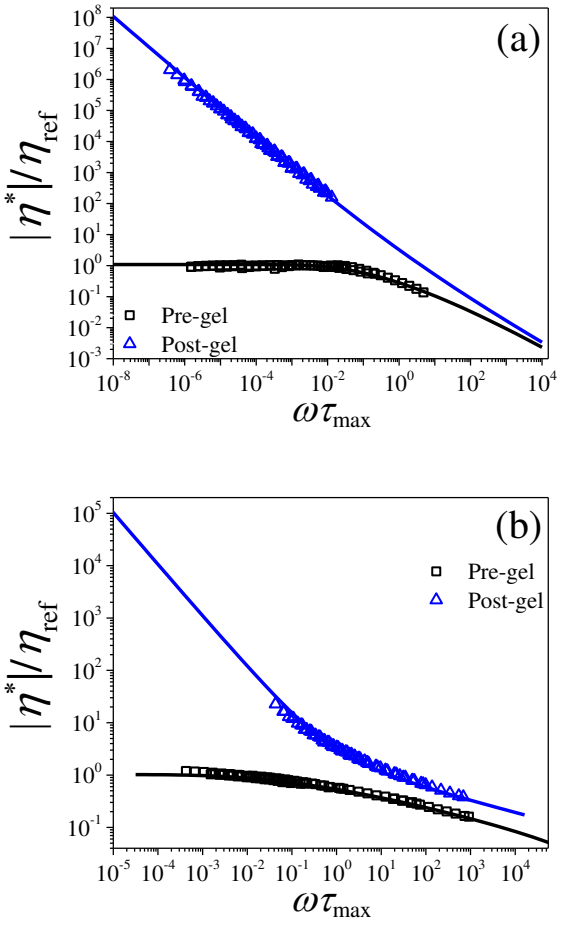


**Figure 7.** Normalized complex viscosity $|\eta^*|$ is plotted as a function of $\omega\tau_{max}$ for (a) colloidal dispersion of hectorite clay at 30°C and (b) PVOH solution. The experimental datapoints are taken from Ref.[19] and shown by symbols while the model fits are shown by solid lines.

The proposed model is observed to be in excellent agreement with the experimental data reported for a spontaneously crosslinking colloidal dispersion at 10°C. However, since the model for $G$ is phenomenological, it is worthwhile to test its generalizability. Thus, the question that animates this section is, "does the proposed model for $G$ describe the viscoelastic functions for any gel-forming system irrespective of nature of gelation, concentration, or temperature?" In an attempt to address this question, we test this model on a variety of gel-forming systems.

To begin with, it is well-known that the kinetics of gel transition for the colloidal dispersion considered here are highly dependent on temperature. On increasing the temperature from 10°C to 30°C, the time needed to achieve critical gel transition reduces significantly. The detailed effect of temperature on the kinetics of gelation can be found elsewhere.[19, 37, 56] Therefore, we test our model on the colloidal dispersion undergoing gel transition at 30°C. We further extend the applicability of the proposed model to a thermo-responsive polymer solution of poly(vinyl alcohol) (PVOH) undergoing sol-gel transition upon cooling. The oscillatory data of the colloidal dispersion at 30°C and the polymer solution is reported by Suman and Joshi.[19] The superposed $|\eta^*|$ is shown by symbols for the colloidal dispersion and the polymer solution in Figure 7 (a) and (b). The estimated values of $S$, $n$, $\eta_0$, $G_e$, $\tau_{\max,S}$ and $\tau_{\max,G}$ are already reported in the previous publication.[19] With the knowledge of the model parameters from the oscillatory data, we compute $|\eta^*|$ using the methodology previously outlined in this work. The reference state is selected in an identical fashion as discussed previously for the colloidal dispersion at 10°C. Fitting parameters for all the systems considered in this work are tabulated in Appendix B. The solid lines in Figure 7 (a) and (b) represent the model fits. Remarkably, it can be seen that the proposed model shows excellent agreement with both sets of experimental data. It is important to note that for the post-gel data, the value of $m$ = floor($n/\kappa$) varies from 1 for the colloidal dispersion to 3 for the PVOH system. This highlights the applicability of the proposed model to any gel-forming system with critical gel state having either elastically dominant (with $n$ = 0.29 for colloidal dispersion) or viscous dominant (with $n$ = 0.79 for polymer solution) characteristics. Very importantly, the colloidal dispersion undergoes spontaneous gelation while the polymer solution undergoes physical gelation upon cooling. Consequently, the relative distance to gelation, analogous to the extent of crosslinking, is expressed in terms of time for the colloidal dispersion ($|p_c - p| \sim |t_g - t|$) and temperature for the PVOH solution (

$|p_c - p| \sim |T_c - T|$, where $T_c$ is the temperature at which the critical gel transition occurs in PVOH solution). The rationale behind such equivalence is discussed by Suman and Joshi.[19] It is, therefore, important to note that irrespective of the gelation variable, the model fits the experimental data exceedingly well for the colloidal dispersion and the polymer solution in Figure 7. This agreement provides further confidence in the validity of the proposed model and methodology for any gel-forming material irrespective of temperature and nature of gelation.

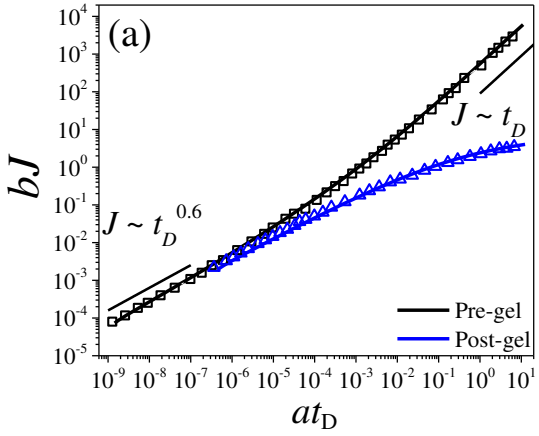


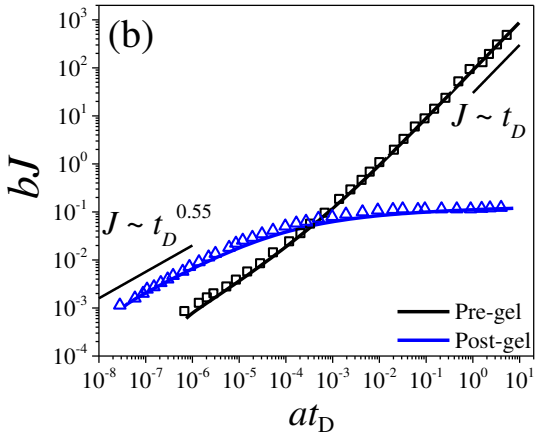

**Figure 8.** Superposed creep compliance ( $J$ ) for (a) peptide and (b) polyacrylamide gels are plotted as a function of lag time ( $t_D$ ). The parameters $a$ and $b$ represent the shift factors used for obtaining the superposition. The symbols are experimental data (square represents pre-gel and triangles represent post-gel state) taken from Ref.[35] and the lines represent fits to the proposed model.

The model parameters of Eqns. (16) to (18) characterize an approach to and from the critical gel state. These parameters can also be obtained through mean squared displacement (MSD) data for a gel-forming system at different extents of gelation. An example of such detailed MSD data is reported by Furst and coworkers[35] for peptide and acrylamide gels. The sol-gel transition in peptide solution proceeds with time while gelation in acrylamide gel occurs with an increase in the crosslinker (bis-acrylamide) concentration. Therefore, the extent of gelation is expressed in terms of time for peptide gel ($|p_c - p| \sim |t_g - t|$) and concentration of the crosslinker ( $c$ ) for acrylamide gel ($|p_c - p| \sim |c_g - c|$ where $c_g$ is the critical concentration of the crosslinker at the point of critical sol-gel transition). Using the MSD data, we obtain the creep compliance using the generalized Stokes-Einstein relation. The computed value of $J$ from the experimental data is plotted as symbols in Figure 8. Furthermore, the parameters $n$ and $S$ are obtained through the MSD data at the critical gel state. The value of $\kappa$ is obtained from the power-law behavior of the shift factors used for superposition. Given values (or guesses) for all the six model parameters, we can numerically obtain $J$ from $G$ using the method described in Appendix A. The values of the unknown parameters ( $\alpha_S$ and $\alpha_G$ ) are obtained by fitting the theoretical $J$ to the experimental data. It is important to note that the fitting parameters $\alpha_S$ and $\alpha_G$ are proportional to $|t - t_g|$ in a similar way as expressed for the colloidal dispersion undergoing spontaneous gelation. However, for the acrylamide gel, the parameters are defined as $\alpha_S = |c_g - c| / C_S^{\kappa}$ and $\alpha_G = |c_g - c| / C_G^{\kappa}$. The best-fit creep compliance parameters are shown in Table 2 in Appendix B. The corresponding curves are shown by solid lines in Figure 8.

The creep compliances obtained from the model show excellent agreement with the experimental data. The value of $m$ varies from 2 for the acrylamide solution data to 3 for the peptide solution data. Furthermore, the growth of $J$ in the pre-gel and post-gel states

approach the power-law behavior given by $n$ in the limit of low lag time ($t_D$). Additionally, the viscous nature of the pre-gel state is also demonstrated by the model prediction by a linear increase in $J$ with $t_D$. This agreement between experimental data and the proposed model for a variety of gel-forming polymers probed using different viscometric functions and with different mechanism of gelation confirms the general nature of the proposed model and hints at its possible universality.

Unlike the clay dispersion and PVOH solution systems reported in Figures 3 and 7, the superposition of the experimental mean-squared displacement for the acrylamide solution and peptide solution used arbitrary shifts. From a practical standpoint, this makes the reference states slightly ambiguous, and the fitting problem insufficiently constrained. This leads to different choices of fitting parameters that end up describing the data equally well. If hyperscaling laws, such as those shown in Figure 2 for the clay dispersion undergoing gelation at 10°C or similar, are established, this uncertainty can be easily resolved. For now, the ability of the phenomenological model to account for the experimental data in Figure 8 demonstrates its flexibility. It is advisable not to over-interpret the corresponding best-fit parameters reported in Table 2 for these systems, with the reassurance that the uncertainty in these parameters can be removed by specifying the experimental data more fully.

The proposed model of $G$ in this work, therefore, leads to the determination of various other viscoelastic properties namely $|\eta^*|$, $H$ and $J$. Furthermore, the proposed form of $G$ in the post-gel state leads to an excellent prediction of the experiment results. This is the first work to obtain the relaxation time spectrum for a gel-forming system at various extent of gelation. Furthermore, the developed model is independent of various factors affecting the gel transition such as temperature. Moreover, the proposed model is validated not only by a colloidal dispersion but is also found to be consistent with polymeric gels, thus highlighting the universality of the proposed model and method. The model parameters can be derived from a simple oscillatory experiment or constant stress experiment. Therefore, our work indicates that a simple model is sufficient to describe the complex rheological response of a gel-forming material.

The sol-gel transition has been observed to take place as a function of different variables such as temperature, the concentration of certain species, time, etc.[3, 4, 14, 18, 19] The spontaneous time-dependent sol-gel transition has been observed in many gel-forming systems such as crosslinking polymeric materials, clay dispersions, PVOH solution, silica

suspension, etc. Among these, when the crosslinking process is due to physical interactions, such as observed in the clay dispersion explored in this work, the spontaneous gelation process increases viscosity as a function of time while the system undergoes a decrease in viscosity under application of sufficiently strong deformation field. In clay dispersions, such a decrease in viscosity is due to the obliteration of interparticle bonds. Particularly in clay dispersions, after cessation of the deformation field, the particles start forming bonds again causing a rise in viscosity, although the system may not pass through the critical gel state.[20] This behavior, wherein a system shows a spontaneous increase in viscosity as a function of time under quiescent conditions and decrease in the same under application of the deformation field, suggests such systems have a thixotropic character. In addition, the post-gel structure of these systems, particularly the clay dispersion, continue to evolve over several months.[57] For the clay dispersion, the corresponding evolution of the properties as a function of time, well beyond the critical state, has been routinely termed as physical aging.[58] It would, therefore, be interesting to study over what timescale in the post-gel state the proposed phenomenological model is applicable.

Although we present a simple phenomenological model, which works well for different kinds of gel-forming systems, there are a few interesting observations that can be explored in future. Based on the different gel-forming systems investigated in the literature and this work, the value of $\kappa$ is narrowly bounded between 0.17-0.28. However, the physical significance behind $\kappa$ adopting a value in the limited range for different gel-forming systems irrespective of the mechanism of gelation, the route to gelation and temperature is still an open question. Furthermore, although the longest relaxation timescale varies symmetrically on either side of the gel state, it is interesting to note that the relaxation time spectrum does not exhibit such symmetry. These aspects deserve more theoretical and experimental investigations, which shall render further insight into this fascinating phenomenon of sol-gel transition.

## 7. Conclusions

The primary goal of this work is to establish a comprehensive phenomenological model for the linear viscoelasticity of systems undergoing a sol-gel transition. It builds on previous work by Scanlan and Winter,[23] which reported expressions for the relaxation modulus in the pre-gel state by augmenting the $G(t)$ corresponding to the critical gel state

with a stretched exponential. Attempts to exploit the symmetry between sol and gel states sought to extend this framework to post-gels by retaining the stretched exponential form but switching the sign of the prefactor. While this could successfully describe the short-time viscoelasticity of systems close to the critical gel state, it led to an unphysical $G(t)$ that was unbounded at long times.

In light of these observations, we proposed a further modification that systematically truncated the Taylor series corresponding to the stretched exponential form proposed by Scanlan and Winter[23] after $m \sim 1$ to 3 terms so that the expression for $G(t)$ is well-behaved. When this is appended to prior expressions for the $G(t)$ of the pre-gel and critical gel states, we obtain a comprehensive 6-parameter phenomenological model for systems undergoing sol-gel transition. We articulated expressions and numerical methods to transform this relaxation modulus to obtain the relaxation time spectra, the frequency response, and the creep compliance. We validated this model on five gel-forming systems that included hectorite clay dispersions, PVOH, acrylamide and peptide solutions. This strongly hints at the potential universality of this model.

Hyperscaling laws for $\eta_0$, $G_e$, $\tau_{\max,S}$ and $\tau_{\max,G}$ as a function of the extent of gelation greatly aided the process of calibrating the phenomenological model. They lead to a unique superposition of the experimental data, while simultaneously expanding its range to several decades of timescales. After reference states are chosen for the pre-gel and post-gel states, this typically leaves only two of the six parameters unspecified. These can be numerically fitted to the superposed data to extract the remaining unknown parameters. The model further expands the reach of experimental characterization, allowing us to make predictions of material behaviour at very short and long timescales that may be inaccessible experimentally. Perhaps, the most attractive feature of a well-calibrated phenomenological model is that it allows us to *fully* characterize *any viscoelastic response* of the material *at any point* in the sol-gel transition.

**Acknowledgements:**

We acknowledge the financial support from the Science and Engineering Research Board (SERB), Government of India. This work is based partially upon work supported by the National Science Foundation under Grant No. DMR 1727870 (S.S).

**Data Availability Statement**

The data that support the findings of this study are available from the corresponding author upon reasonable request.

**Appendix A: Numerical determination of Creep Compliance from Relaxation Modulus**

We begin with the method described in Ref. [55] which starts by numerically approximating the convolution integral at a point $t_i$ as:

$$t_i \approx \sum_{j=1}^{i} J\left(t_{j-1/2}\right) \int_{t_{j-1}}^{t_j} G\left(t_j - \tau\right) d\tau = \sum_{j=1}^{i} J\left(t_{j-1/2}\right) \left( \frac{G\left(t_i - t_j\right) + G\left(t_i - t_{j-1}\right)}{2} \right) \left(t_j - t_{j-1}\right), \tag{A1}$$

where $t_{j-1/2} = \left(t_j + t_{j-1}\right)/2$ is the midpoint of the interval $\left[t_{j-1}, t_j\right]$, and the trapezoidal rule is used to evaluate the integral over the relaxation modulus in the second step. The creep compliance $J(t)$ can be evaluated at $N$ discrete points by solving a lower triangular linear system $Ax = b$, with $x_i = J\left(t_{i-1/2}\right)$, and $b_i = 2t_i$ for $i = 1, \cdots, N$. The triangular matrix $A$ is given by:

$$A_{ij} = \begin{cases} \left( G\left(t_i - t_j\right) + G\left(t_i - t_{j-1}\right) \right) \left(t_j - t_{j-1}\right) & j \le i \\ 0 & j > i \end{cases}. \tag{A2}$$

Since we know the analytical form of $G(t)$ in the pre-gel and post-gel states, we can avoid the trapezoidal rule, and evaluate the integral $\int_{t_{j-1}}^{t_j} G\left(t_i - \tau\right) d\tau$ analytically. For the pre-gel state, setting $\xi_1 = (1-n)/\kappa$ and $\xi_2 = \kappa\alpha^{\xi_1}/S$ for brevity, leads to a linear system $Ax = b$ with $x_i = J\left(t_{i-1/2}\right)$ as before, and $b_i = \xi_2 t_i$. The matrix $A$ is given by:

$$A_{ij} = \begin{cases} \Gamma\left(\xi_1, \alpha(t_i - t_j)^{\kappa}\right) - \Gamma\left(\xi_1, \alpha(t_i - t_{j-1})^{\kappa}\right) & j \le i \\ 0 & j > i \end{cases}. \tag{A3}$$

Here, $\Gamma(a,x) = \int_x^{\infty} t^{a-1} e^{-t}\, dt$ is the upper incomplete gamma function. For the post-gel state, this leads to a triangular system with $x_i = J\left(t_{i-1/2}\right)$, $b_i = t_i$, and

$$A_{ij} = \begin{cases} G_e \times \left(t_j - t_{j-1}\right) + \sum_{k=1}^{m} \frac{S_k}{k!} \frac{(t_i - t_{j-1})^{1-n_k} - (t_i - t_j)^{1-n_k}}{1-n_k} & j \le i \\ 0 & j > i \end{cases} . \quad \text{(A4)}$$

**Appendix B: Best-fit Phenomenological Model Parameters**

We fit the parameters of the phenomenological model for five different systems. The values of the best-fit parameters are listed in Table 2. The curves corresponding to these fitting parameters are reported in Figures 3, 7, and 8. In addition to the six model parameters, $m$ = floor($n/\kappa$) is also shown. For the first three systems, the unique superposition of the complex viscosity shown in Figures 3 and 7 was obtained using the method described in the text and Ref [19]. The extent of gelation in the reference state for the sol corresponded to $\tau_{\max,S} = 1$. The same extent of gelation was used in the reference state for the post-gel state. This effectively fixed all the parameters, except $\alpha_S$ and $\alpha_G$, which are shown in the last two columns.

**Table 2:** The parameters of the phenomenological model used to fit superposed experimental data. The curves corresponding to these fitting parameters are reported in Figures 3, 7, and 8.

| System [source of the data] | $S$ $\left[\text{Pa.s}^n\right]$ | $n$ | $\kappa$ | $m$ | $G_e$ [Pa] | $\alpha_G$ $\left[1/s^\kappa\right]$ | $\alpha_S$ $\left[1/s^\kappa\right]$ |
|---|---|---|---|---|---|---|---|
| Aq. Clay dispersion 10°C [This work] | 3.80 | 0.35 | 0.19 | 1 | 9.14 | 0.2 | 2.1 |
| Aq. Clay dispersion 30°C [Ref [19]] | 4.35 | 0.29 | 0.17 | 1 | 5.38 | 1.2 | 2.4 |
| Aq. PVOH solution [Ref [19]] | 0.54 | 0.79 | 0.20 | 3 | 8.00 | 1.4 | 0.9 |
| Aq. Acrylamide solution [Ref [35]] | 0.14 | 0.58 | 0.28 | 2 | 30.0 | 20 | 17 |
| Aq. Peptide Solution with bis-acrylamide crosslinker [Ref [35]] | 0.03 | 0.60 | 0.20 | 3 | 0.01 | 2.8 | 9.0 |

For the aqueous acrylamide solution and aqueous peptide solutions, arbitrary shift factors were used to obtain the superposition of the mean-squared displacement in the original

dataset (Ref [35]). Since hyper-scaling laws and reference states are not clearly established (unlike the first three datasets reported in Table 2) the fitting problem is insufficiently constrained. This is particularly true for the post-gel response where different combinations of $G_e$ and $\alpha_G$ can describe the data equally well.

**References:**

1. L. L. Hench, and J. K. West, "The sol-gel process," Chemical reviews **90**, 33 (1990).
2. J. Rouwhorst, C. Ness, S. Stoyanov, A. Zaccone, and P. Schall, "Nonequilibrium continuous phase transition in colloidal gelation with short-range attraction," Nature Communications **11**, 3558 (2020).
3. A. S. Negi, C. G. Redmon, S. Ramakrishnan, and C. O. Osuji, "Viscoelasticity of a colloidal gel during dynamical arrest: Evolution through the critical gel and comparison with a soft colloidal glass," Journal of Rheology **58**, 1557 (2014).
4. S. Liu, W. L. Chan, and L. Li, "Rheological properties and scaling laws of κ-carrageenan in aqueous solution," Macromolecules **48**, 7649 (2015).
5. E. R. Morris, K. Nishinari, and M. Rinaudo, "Gelation of gellan – A review," Food Hydrocolloids **28**, 373 (2012).
6. H. E.Park, N. Gasek, JadenHwang, D. J. Weiss, and P. C.Lee, "Effect of temperature on gelation and cross-linking of gelatin methacryloyl for biomedical applications," Physics of Fluids **32**, 033102 (2020).
7. J. DongPark, and S. A. Rogers, "Rheological manifestation of microstructural change of colloidal gel under oscillatory shear flow," Physics of Fluids **32**, 063102 (2020).
8. S. Kumar, N. E. Prasad, and Y. M. Joshi, "Crosslinking Reaction Under a Stress and Temperature Field: Effect on Time-Dependent Rheological Behavior During Thermosetting Polymer Processing," ACS Applied Polymer Materials (2019).
9. C. H. Lee, Y. Lu, and A. Q. Shen, "Evaporation induced self assembly and rheology change during sol-gel coating," Physics of Fluids **18**, 052105 (2006).
10. T. Yoshida, Y. Tasaka, and P. Fischer, "Ultrasonic spinning rheometry test on the rheology of gelled food for making better tasting desserts," Physics of Fluids **31**, 113101 (2019).
11. K. Haldar, and S. Chakraborty, "Investigation of chemical reaction during sodium alginate drop impact on calcium chloride film," Physics of Fluids **31**, 072102 (2019).
12. J. E. Martin, and J. P. Wilcoxon, "Critical dynamics of the sol-gel transition," Physical review letters **61**, 373 (1988).
13. H. Watanabe, T. Sato, K. Osaki, Y. Aoki, L. Li, M. Kakiuchi, and M.-L. Yao, "Rheological images of poly (vinyl chloride) gels. 4. Nonlinear behavior in a critical gel state," Macromolecules **31**, 4198 (1998).
14. H. H. Winter, and M. Mours, "Rheology of Polymers Near Liquid-Solid Transitions," Advances in Polymer Science **134**, 165 (1997).
15. M. Mours, and H. H. Winter, "Time-resolved rheometry," Rheologica Acta **33**, 385 (1994).
16. K. Suman, and Y. M. Joshi, "Analyzing onset of nonlinearity of a colloidal gel at the critical point," Journal of Rheology **63**, 991 (2019).
17. H. H. Winter, and F. Chambon, "Analysis of Linear Viscoelasticity of a Crosslinking Polymer at the Gel Point," Journal of Rheology **30**, 367 (1986).
18. A. Zaccone, H. Winter, M. Siebenbürger, and M. Ballauff, "Linking self-assembly, rheology, and gel transition in attractive colloids," Journal of Rheology **58**, 1219 (2014).

19. K. Suman, and Y. M. Joshi, "On the universality of the scaling relations during sol-gel transition," Journal of Rheology **64**, 863 (2020).
20. S. Jatav, and Y. M. Joshi, "Rheological signatures of gelation and effect of shear melting on aging colloidal suspension," Journal of Rheology **58**, 1535 (2014).
21. H. H. Winter, "Evolution of rheology during chemical gelation," Progress in Colloid & Polymer Science **75**, 104 (1987).
22. M. Baumgaertel, and H. H. Winter, "Determination of discrete relaxation and retardation time spectra from dynamic mechanical data," Rheologica Acta **28**, 511 (1989).
23. J. C. Scanlan, and H. H. Winter, "The evolution of viscoelasticity near the gel point of end-linking poly(dimethylsiloxane)s," Makromolekulare Chemie. Macromolecular Symposia **45**, 11 (1991).
24. K. Suman, and Y. M. Joshi, "Microstructure and Soft Glassy Dynamics of an Aqueous Laponite Dispersion," Langmuir **34**, 13079 (2018).
25. D. Stauffer, A. Coniglio, and M. Adam, "Gelation and critical phenomena," Advances in Polymer Science **44**, 103 (1982).
26. P.-G. de Gennes, *Scaling concepts in polymer physics* (Cornell university press, Ithaca, New York, 1979).
27. M. Gordon, and S. B. Ross-Murphy, "The graph-like state of matter XI. Electrical conductivity of random networks, gelation and elasticity," Journal of Physics A: Mathematical and General **11**, L155 (1978).
28. S. Kirkpatrick, "The nature of percolation 'channels'," Solid State Communications **12**, 1279 (1973).
29. D. Stauffer, "Gelation in concentrated critically branched polymer solutions. Percolation scaling theory of intramolecular bond cycles," Journal of the Chemical Society, Faraday Transactions 2: Molecular and Chemical Physics **72**, 1354 (1976).
30. J. E. Martin, D. Adolf, and J. P. Wilcoxon, "Viscoelasticity of Near-Critical Gels," Physical Review Letters **61**, 2620 (1988).
31. M. F. Thorpe, "Continuous deformations in random networks," Journal of Non-Crystalline Solids **57**, 355 (1983).
32. H. He, and M. F. Thorpe, "Elastic Properties of Glasses," Physical Review Letters **54**, 2107 (1985).
33. A. Zaccone, and E. Scossa-Romano, "Approximate analytical description of the nonaffine response of amorphous solids," Physical Review B **83**, 184205 (2011).
34. A. Zaccone, "Elastic deformations in covalent amorphous solids," Modern Physics Letters B **27**, 1330002 (2013).
35. T. H. Larsen, and E. M. Furst, "Microrheology of the Liquid-Solid Transition during Gelation," Physical Review Letters **100**, 146001 (2008).
36. M. A. V. Axelos, and M. Kolb, "Crosslinked biopolymers: Experimental evidence for scalar percolation theory," Physical Review Letters **64**, 1457 (1990).
37. S. Jatav, and Y. M. Joshi, "Phase Behavior of Aqueous Suspension of Laponite: New Insights with Microscopic Evidence," Langmuir **33**, 2370 (2017).
38. S. K. Venkataraman, and H. H. Winter, "Finite shear strain behavior of a crosslinking polydimethylsiloxane near its gel point," Rheologica Acta **29**, 423 (1990).
39. M. Kaushal, and Y. M. Joshi, "Validation of Effective Time Translational Invariance and Linear Viscoelasticity of Polymer Undergoing Cross-linking Reaction," Macromolecules **47**, 8041 (2014).
40. G. Yin, and M. J. Solomon, "Soft glassy rheology model applied to stress relaxation of a thermoreversible colloidal gel," Journal of Rheology **52**, 785 (2008).
41. R. Bandyopadhyay, P. H. Mohan, and Y. M. Joshi, "Stress relaxation in aging soft colloidal glasses," Soft Matter **6**, 1462 (2010).

42. R. Milkus, and A. Zaccone, "Atomic-scale origin of dynamic viscoelastic response and creep in disordered solids," Physical Review E **95**, 023001 (2017).
43. M. Baumgaertel, and H. H. Winter, "Interrelation between continuous and discrete relaxation time spectra," Journal of Non-Newtonian Fluid Mechanics **44**, 15 (1992).
44. A. Takeh, and S. Shanbhag, "A Computer Program to Extract the Continuous and Discrete Relaxation Spectra from Dynamic Viscoelastic Measurements," Applied Rheology **23**, 24628 (2013).
45. J. D. Ferry, *Viscoelastic properties of polymers* (John Wiley & Sons, New York, 1980).
46. P. Virtanen, R. Gommers, T. E. Oliphant, M. Haberland, T. Reddy, D. Cournapeau, E. Burovski, P. Peterson, W. Weckesser, J. Bright, S. J. van der Walt, M. Brett, J. Wilson, K. J. Millman, N. Mayorov, A. R. J. Nelson, E. Jones, R. Kern, E. Larson, C. J. Carey, İ. Polat, Y. Feng, E. W. Moore, J. VanderPlas, D. Laxalde, J. Perktold, R. Cimrman, I. Henriksen, E. A. Quintero, C. R. Harris, A. M. Archibald, A. H. Ribeiro, F. Pedregosa, P. van Mulbregt, A. Vijaykumar, A. P. Bardelli, A. Rothberg, A. Hilboll, A. Kloeckner, A. Scopatz, A. Lee, A. Rokem, C. N. Woods, C. Fulton, C. Masson, C. Häggström, C. Fitzgerald, D. A. Nicholson, D. R. Hagen, D. V. Pasechnik, E. Olivetti, E. Martin, E. Wieser, F. Silva, F. Lenders, F. Wilhelm, G. Young, G. A. Price, G.-L. Ingold, G. E. Allen, G. R. Lee, H. Audren, I. Probst, J. P. Dietrich, J. Silterra, J. T. Webber, J. Slavič, J. Nothman, J. Buchner, J. Kulick, J. L. Schönberger, J. V. de Miranda Cardoso, J. Reimer, J. Harrington, J. L. C. Rodríguez, J. Nunez-Iglesias, J. Kuczynski, K. Tritz, M. Thoma, M. Newville, M. Kümmerer, M. Bolingbroke, M. Tartre, M. Pak, N. J. Smith, N. Nowaczyk, N. Shebanov, O. Pavlyk, P. A. Brodtkorb, P. Lee, R. T. McGibbon, R. Feldbauer, S. Lewis, S. Tygier, S. Sievert, S. Vigna, S. Peterson, S. More, T. Pudlik, T. Oshima, T. J. Pingel, T. P. Robitaille, T. Spura, T. R. Jones, T. Cera, T. Leslie, T. Zito, T. Krauss, U. Upadhyay, Y. O. Halchenko, Y. Vázquez-Baeza, and C. SciPy, "SciPy 1.0: fundamental algorithms for scientific computing in Python," Nature Methods **17**, 261 (2020).
47. H. Winter, "Can the gel point of a cross-linking polymer be detected by the G′–G ″crossover?," Polymer Engineering & Science **27**, 1698 (1987).
48. S. Shanbhag, "pyReSpect: A Computer Program to Extract Discrete and Continuous Spectra from Stress Relaxation Experiments," Macromolecular Theory and Simulations **28**, 1900005 (2019).
49. A. P. R. Eberle, R. Castañeda-Priego, J. M. Kim, and N. J. Wagner, "Dynamical Arrest, Percolation, Gelation, and Glass Formation in Model Nanoparticle Dispersions with Thermoreversible Adhesive Interactions," Langmuir **28**, 1866 (2012).
50. T. S. Ng, and G. H. McKinley, "Power law gels at finite strains: the nonlinear rheology of gluten gels," Journal of Rheology **52**, 417 (2008).
51. S. W. Park, and R. A. Schapery, "Methods of interconversion between linear viscoelastic material functions. Part I—a numerical method based on Prony series," International Journal of Solids and Structures **36**, 1653 (1999).
52. R. J. Loy, F. R. de Hoog, and R. S. Anderssen, "Interconversion of Prony series for relaxation and creep," Journal of Rheology **59**, 1261 (2015).
53. N. W. Tschoegl, *The phenomenological theory of linear viscoelastic behavior* (Springer, Berlin, 1989).
54. P. J. Dooling, C. P. Buckley, and S. Hinduja, "An intermediate model method for obtaining a discrete relaxation spectrum from creep data," Rheologica Acta **36**, 472 (1997).
55. J. Sorvari, and M. Malinen, "Numerical interconversion between linear viscoelastic material functions with regularization," International Journal of Solids and Structures **44**, 1291 (2007).
56. K. Suman, and Y. M. Joshi, "Kinetic model for a sol-gel transition: application of the modified Bailey criterion," Rheologica Acta (2020).

57. P. Mongondry, J. F. Tassin, and T. Nicolai, "Revised state diagram of Laponite dispersions," J.Colloid Interface Sci. **283**, 397 (2005).
58. A. Shukla, S. Shanbhag, and Y. M. Joshi, "Analysis of linear viscoelasticity of aging soft glasses," Journal of Rheology **64**, 1197 (2020).